JOURNAL OF MATERIALS SCIENCE 26 (1991) 3438–3448

Analysis of three-dimensional textile preforms for multidirectional reinforcement of composites

GUANG-WU DU*, TSU-WEI CHOU‡
*Center for Composite Materials,‡ and also Department of Mechanical Engineering, University of Delaware, Newark, DE 19716, USA

P. POPPER
Engineering Technology Laboratory, E. I. du Pont de Nemours and Co., Wilmington, DE 19880-0304, USA

A mathematical model has been developed to describe the structural geometry of three-dimensional textile preforms made by the two-step braiding process. These structures consist of parallel yarns, interconnected with braiding yarns, that lie in complex spatial orientations. The model predicts structural features such as fibre orientation, fibre volume fraction, and interyarn voids from the key process variables of braiding pattern, advance rate, and yarn geometry. The limiting geometry was computed by establishing the point at which yarns jam against each other. Using this factor makes it possible to identify the complete range of allowable geometric arrangements for this type of preform. Experiments of several bare and impregnated samples confirmed the theoretical predictions and demonstrated that very high fibre loadings (above 75% fibre volume fraction) could be achieved. The modelling technique used a "unit cell" approach, which can be applied to many other types of preform for advanced composites.

Nomenclature

- κ fibre packing fraction (fibre-to-yarn area ratio)
- N_r number of rings in idealized yarn with open packing
- N_f number of filaments in yarn
- f_a aspect ratio of axial yarns (as defined in Equation 3)
- f_b aspect ratio of braiders (thickness to width)
- f aspect ratio of braid completed (thickness to width)
- γ angle of braider yarns to braid surface (in end projection)
- S yarn dimension (m)
- t braid thickness (m)
- w braid width (m)
- m number of axial columns
- n number of axial layers
- α angle of braider yarn to axial yarn (braider yarn orientation)
- h pitch length for two braiding steps (m)
- λ yarn linear density (kg m^{-1})
- ρ fibre density (kg m^{-3})
- L_b length of braider in a unit cell (m), P1 to P2 in Fig. 6;
- L_p projected length of L_b (m)
- V volume of yarn or void component in a unit cell (m^3)
- v_f fibre volume fraction – all fibres to total volume
- v_b braider volume fraction – braider fibres to total fibres
- v_v void volume fraction – interyarn voids to total volume

Subscripts

- o refers to theoretical open packing
- c refers to theoretical close packing
- a refers to axial yarns
- b refers to braiders
- m, n refer to axial yarns on braid face (see Fig. 5)
- t refers to total unit cell
- j refers to jamming point

1. Introduction

A number of three-dimensional fabrics, sometimes referred to as preforms, have been developed for reinforcing composites. These fabrics, which can be made quite thick (up to about 0.5 m), offer advantages over conventional weaves that are layered to form composites. The three-dimensional fabrics provide enhanced properties and the possibility for near-net-shape reinforcement.

A key property of three-dimensional fabrics is their ability to reinforce composites in the thickness direction. Unlike conventional laminates, three-dimensional

0022–2461/91 $03.00 + .12 © 1991 Chapman and Hall Ltd.

fabrics include fibres that interconnect layers and are oriented at angles to the plane of the composite. This construction reduces the usual tendency toward delamination. Perhaps the most important feature of the three-dimensional fabrics is the possibility of fabricating a wide range of complex shapes ranging from solid rods to I-beams and thick-walled rocket nozzles. Making these shapes integrally, rather than from layers, eliminates the need for cutting fibres to form joints, splices, or overlaps with the associated local strength loss. Direct formation of integral shapes also offers the possibility of greatly simplifying the composite's manufacturing process.

Other methods of reinforcing composites, such as filament winding, also provide near net shapes. However, only fabric preforms fully interconnect the fibrous array to provide both through-thickness properties and a "stand alone" structure that is stable without a matrix.

Processes for making three-dimensional fabrics continue to be developed. The principal methods include variations of the traditional textile processes of weaving, knitting, and braiding.

Weaving can be done by using either conventional looms with multilayer constructions or entirely new equipment. Knitting can be used to interconnect fibre arrays that have been arranged by other techniques. Knitting can also be used to create shapes (by methods similar to those used in making sweaters). Braiding can form shapes either by overbraiding mandrels in conventional circular machines or by using new braiding patterns to form solid shapes directly.

Three-dimensional braids have been produced on traditional horn-gear machines for ropes and packings in solid, circular, or square cross-sections. However, this type of machine uses only a small number of yarn carriers (≤ 24) and cannot form complex shapes. Their applicability to composites is therefore limited. A number of new machines without the traditional horn gears have been developed to create complex shapes. The new braiding processes include: two-step [1], AYPEX [2], interlock twiner [3], and row and column [4] (also referred to as omiweave, magnaweave, through-the-thickness, and four-step, respectively, in the literature).

The analysis presented in this paper applies to the two-step braid. This structure includes a large number of parallel (axial) yarns aligned with the basic structure for efficient reinforcement and a smaller number of braiding yarns (braiders) that form the shape and interconnect the fabric.

A generalized schematic of a three-dimensional braiding process is shown in Fig. 1. Axial yarns, if present in a particular braid, are fed directly into the structure from packages located below the track plate. Braiding yarns are fed from bobbins mounted on carriers that move on the track plate. The pattern of motion of the braiders relative to each other and the axial yarns establishes the type of braid being formed, as well as the microstructure.

In the two-step braid, the braiders move according to the pattern shown in Fig. 2. They are arranged around the perimeter of an axial array as shown. It is important to note that this axial array can be arranged in essentially any shape, including I-beams, box beams, circular tubes, and others. In each case, the braiders move through the axial array in two sequential steps as shown. In the first, the braiders all move in one diagonal line but in alternating directions. In the second, they move along the other diagonal as shown.

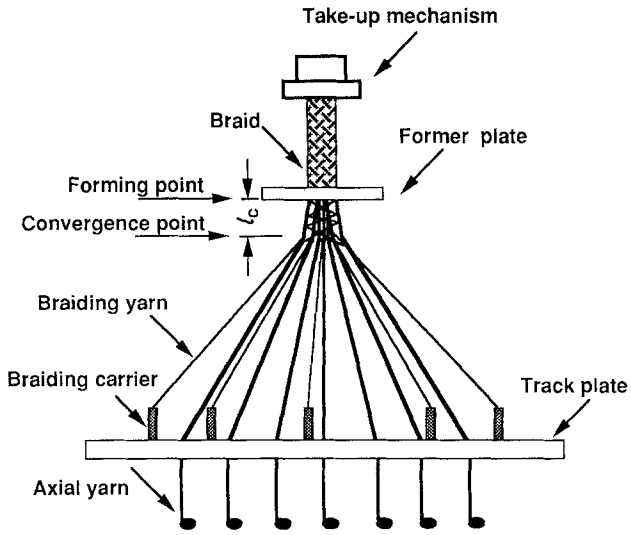

Figure 1 Schematic drawing of a two-step braider.

Although the machine action consists of only two steps, each braider moves through a large portion or even all of the structure. This can be seen by tracing the path of a single braider subjected to the repeated two steps of machine action shown in Fig. 2. The paths followed by all braiders will completely intercinch the axial yarns and lock them in the desired shape.

Compared with other three-dimensional braiding processes, two-step braiding has several distinct advantages. A relatively simple sequence of braider motions can form a wide range of shapes. During each step of the process, all the braiders are simultaneously outside of the axial array, and it is then possible to add various inserts to the structure or even rearrange the axial array geometry. Furthermore, this structure can be made with a high level of fibre packing, as will be shown, and it includes a large number of axially oriented fibres as needed in many applications.

The two-step process has motivated a number of researchers and these studies have been reported. El Shiekh and Li modelled the microgeometry using idealized circular yarns [5]. Several investigators have evaluated the mechanical properties of consolidated two-step composites [6, 7]. The present paper includes a microgeometric model of this structure based on experimental observations. Measurements are also made to confirm the basic theory proposed.

2. Analysis

Our analysis provides the basic description of the microgeometry of two-step braids. The key inputs are (1) the size, type, and shape of each of the two yarns used, braiders and axial yarns; (2) the braid pattern (size of axial array); and (3) the advance rate during

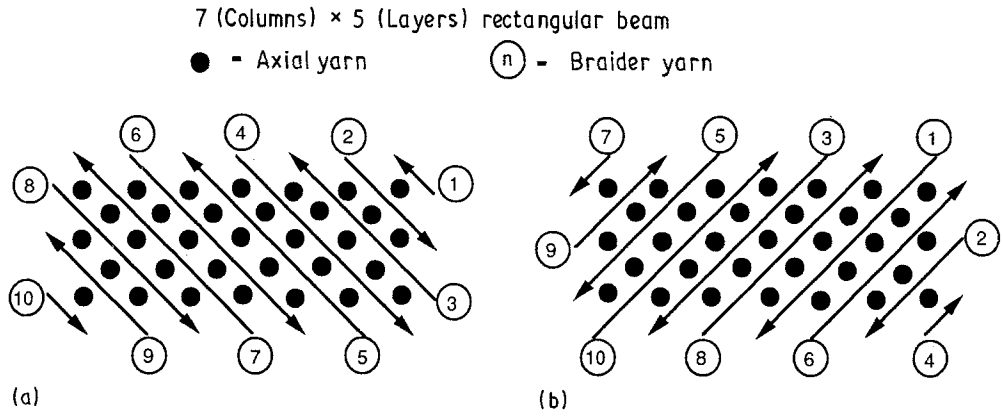

Figure 2 Two-step braiding pattern showing the relative motion of yarns. (a) Step 1, (b) Step 2.

braiding. The key outputs are braid dimensions, fibre orientation, interyarn void content, fibre volume fraction, and geometric limits imposed by yarns jamming against each other.

Although shaped parts are of greatest interest for this type of structure, the analysis has been done on a rectangular cross-section. We believe that the results of this relatively simple structure provide approximate solutions for shaped parts. The methodology developed here regarding yarn cross-sections, unit cells, and yarn jamming can be used to analyse more complex shapes, as well as other types of three-dimensional fabrics.

2.1. Assumptions and limitations

1. Multifilament yarns are used for both braiders and axial yarns. These yarns are made of a large number of filaments, and they can readily deform their cross-sections to prismatic shapes as they flatten against each other.
2. Round filament cross-section.
3. Filaments are parallel along the yarn length, i.e. zero twist.
4. Yarn tensions are high enough to ensure straight yarn path, except for the braider yarns, which are bent around the braid surface.
5. Inextensible filaments.
6. Rectangular braid shape with low aspect ratio – thickness to width.

2.2. Packing of fibres in a yarn

The fibre volume fraction of a three-dimensional fabric depends on the level to which yarns pack against each other in the structure and the level that fibres pack against each other in a yarn. In this section, we describe two methods for estimating interfibre packing, using methods reported in the textile literature; a later section covers yarn packing in the fabric.

The geometry of interfibre packing in yarns has been studied by a number of researchers primarily for textile applications [8]. Two basic idealized packing forms were identified: open packing, in which the fibres are arranged in concentric layers, as illustrated in Fig. 3a; and close packing, in which the fibres are arranged in a hexagonal pattern as in Fig. 3b.

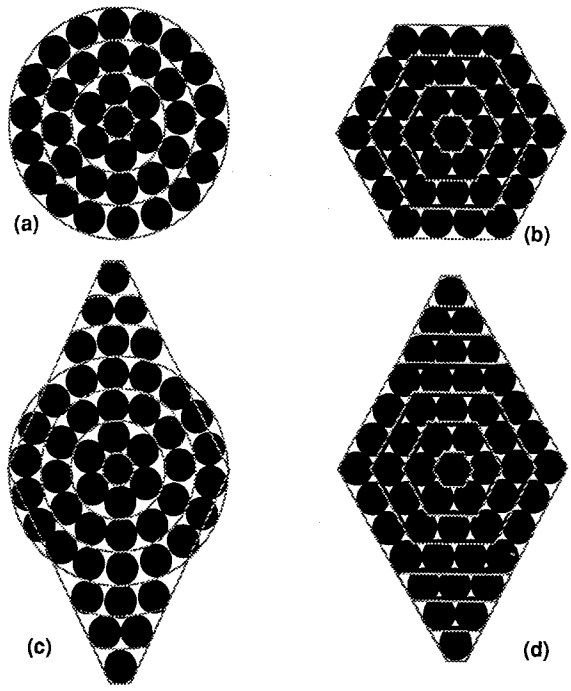

Figure 3 Fibre packing in yarns: (a) open-packing in circular yarns; (b) close-packing in hexagonal yarns; (c) open-packing in diamond-shaped yarn; (d) close-packing in diamond-shaped yarn.

In open-packed yarns the packing fraction, defined as fibre to yarn area ratio, has been computed as a function of the number of fibres. If the outer ring is completely filled and the fibres are circular, the packing fraction can be shown to equal

$$\kappa_o = \frac{3N_r(N_r - 1) + 1}{(2N_r - 1)^2} \quad (1)$$

where N_r is the number of rings and its relationship to the number of yarns, N_f, is given by

$$N_r = \frac{1}{2} + \left[\frac{1}{4} + \frac{1}{3}(N_f - 1)\right]^{1/2} \quad (2)$$

For large numbers of fibres this packing fraction approaches 0.75.

In close-packed yarns, for any number of circular fibres if the outer layer is completely filled, the packing

fraction can be shown to equal the area ratio of a circle to an enclosing hexagon.

$$\kappa_c = \frac{\pi}{2.3^{1/2}} = 0.91 \quad (3)$$

The level of packing fraction predicted by the two models assumed circular and hexagonal yarns, respectively. However, as shown in Fig. 3c and d, they apply equally well to other shapes if the number of fibres is sufficiently large.

In addition to the level of packing fraction, the fibres also establish the yarn cross-sectional shape, i.e. yarn packing in fabrics. This shape plays a significant role in determining how many fibres can be packed into a fabric. In the textile literature, the yarns are often assumed to have a circular cross-section [9, 10]. However, it has been shown that even highly twisted yarns deviate significantly from circularity and the yarn cross-section varies considerably for different types of fabric. Many attempts have been made to develop more realistic geometrical models for fabrics by assuming shapes such as elliptical and race-track sections [11].

In the experimental phase of this study, discussed in a later section, we found that the yarns in two-step braids tend to be prismatic. The axial yarns have diamond cross-sections and the braiders are rectangular. The packing fraction was measured to be 0.78, after consolidation for all yarns. This level lies between the predicted levels of 0.75 and 0.91. The observed yarn shapes were used to develop the fabric geometry model.

Factors that affect both fibre and yarn packing include yarn tension, interyarn contact, yarn twist, fibre cross-section, fibre straightness, manufacturing method, and fabric geometry. Precise description of actual fibre packing in a particular yarn and yarn packing in a particular fabric is possible only from experimental observations.

2.3. Yarn cross-section

The previous section dealt with the number of fibres that can be packed in a yarn. In this section, we develop a model for the yarn cross-section as it occurs in two-step braids. The model assumes that the yarns have cross-sections as shown in Fig. 4 directly after

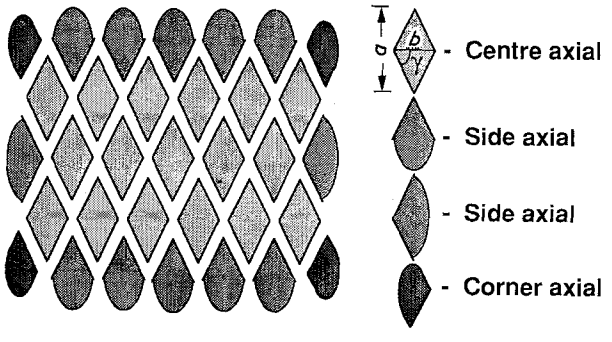

Figure 4 Cross-sections of axial yarns in a rectangular braided preform before consolidation.

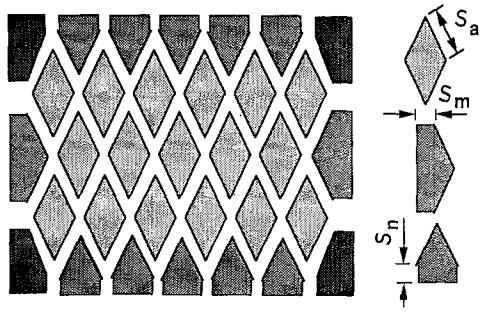

Figure 5 Cross-sections of axial yarns in a rectangular braided consolidated composite.

braiding. After matrix addition and consolidation, the fabric is assumed to be flattened as shown on Fig. 5. The axial yarn cross-section depends on its location in the fabric. Central yarns, which form the bulk of the structure, are diamond shaped. Axial yarns on the side and corners of the structure are pentagonal as shown. Braiding yarns, which are not shown in Figs 4 and 5 for reason of clarity, are assumed to be rectangular.

In our experiments we found that yarn cross-sections corresponded closely to the assumed shapes of Figs 4 and 5.

The aspect ratio of axial yarns, f_a, is related to the inclination angle of the braiders to the fabric plane by

$$f_a = \frac{a}{b} = \tan\gamma \quad (4)$$

This aspect ratio, f_a, can vary significantly because of braider yarn tension or external compression applied at the forming point during the process. It can also be changed by compacting the entire braided preform to a specified braid aspect ratio f before or during resin impregnation. These aspect ratios affect the shape of the final braid (macrogeometry) as well as the braider yarn orientation angle, α, and fibre volume fraction, v_f (microgeometry).

With unit axial aspect ratio ($\gamma = \pi/4$), the cross-section of the centre axial yarns becomes square. In this special case, as will be shown, the fibre volume fraction is at a maximum.

The axial yarn dimensions can be calculated from the cross-section of the consolidated braid in Fig. 5. These relations are given in terms of yarn area and inclination angle. The yarn area is in turn evaluated from its linear density and the fibre packing fraction and density.

$$S_a = \left[\frac{\lambda_a}{\rho_a \kappa_a \sin(2\gamma)}\right]^{1/2} \quad (5)$$

$$S_n = \frac{\lambda_n - 0.5\lambda_a}{2S_a \rho_a \kappa_a \cos\gamma} \quad (6)$$

$$S_m = \frac{\lambda_m - 0.5\lambda_a}{2S_a \rho_a \kappa_a \sin\gamma} \quad (7)$$

The parameters λ_a, λ_m and λ_n are the linear density of the centre and both "side" axial yarns, ρ_a is the fibre density, and κ_a is the packing fraction. The assumptions of $\lambda_m \geq 0.5\lambda_a$ and $\lambda_n \geq 0.5\lambda_a$ are implied in the

expressions above to ensure positive values of S_m and S_n. Also, the packing fraction κ_a is assumed to be constant for all axial yarns.

The braiding yarns are shown in Fig. 6 for two steps of the braiding pattern as indicated. These yarns are assumed to be rectangular with aspect ratio, f_b. The aspect ratio is usually much less than unity because of compression by the axial yarns. Its level can be adjusted by such factors as yarn tension and lateral compliance. The dimension of a braider yarn can also be calculated from its packing fraction (κ_b), yarn linear density (λ_b), and fibre density (ρ_b).

$$S_b = \left[\frac{\lambda_b}{\rho_b \kappa_b f_b}\right]^{1/2} \quad (8)$$

2.4. Model of a unit cell of the three-dimensional fabric

In this section we develop the basic relations of macro and microgeometry for the rather complex three-dimensional structure of two-step braids. The key outputs are the fibre orientation and the volume of each component – braiding yarns, axial yarns, and interyarn voids.

This computation employs the technique of a "unit cell", which repeats throughout the structure. In many fabrics such a unit cell is readily identified, but in fabrics of this complexity it can be very difficult to define. Fig. 7 shows the unit cell identified for this analysis. There are four such symmetrical cells, labelled A–D, which repeat as a group. Because of the symmetry, any one can be used to find the required relations.

The length of the unit cell in Fig. 7 is the length of braid formed in one of the two machine steps. This length is actually half of the fabric pitch length, as shown in Figs 6–9. Five layers are shown in Fig. 7, but the computation permits an arbitrary number to be used. The number of columns, however, has been assumed to be very large so that the rather complicated edge effects can be avoided. Fig. 8 shows the difference between finite and infinite columns and the effect on braider paths.

The width and thickness of the braided preform can be computed from Figs 5 and 6 in terms of the basic input variables. Note that, in this portion of the computation, the restriction of infinite numbers of columns is not imposed. The resulting relations can be shown to equal

$$w = (m - 1)\frac{S_a}{\sin\gamma}\psi_w \quad (9)$$

$$t = \frac{n - 1}{2}\frac{S_a}{\cos\gamma}\psi_t \quad (10)$$

where

$$\psi_w = \sin(2\gamma) + \frac{f_b S_b}{S_a} + \frac{\lambda_m - 0.5\lambda_a}{S_a^2 \rho_a \kappa_a}\frac{1}{m - 1} \quad (11)$$

$$\psi_t = \sin(2\gamma) + \frac{f_b S_b}{S_a} + \frac{\lambda_n - 0.5\lambda_a}{S_a^2 \rho_a \kappa_a}\frac{2}{n - 1} \quad (12)$$

From Equations 9 and 10, the aspect ratio of the braided preform can be obtained

$$f = \frac{t}{w} = \frac{1}{2} f_a \frac{n - 1}{m - 1}\frac{\psi_t}{\psi_w} \quad (13)$$

An important special case exists if the linear density of each side axial yarn (λ_m and λ_n) equals half that of the centre axial yarns (λ_a). In that case, $\psi_t = \psi_w$ and Equation 13 simplifies to

$$f = \frac{1}{2} f_a \frac{n - 1}{m - 1} \quad (14)$$

With a known or preset f, the aspect ratio of axial yarns, f_a, can be calculated from Equation 13 or estimated from Equation 14.

The braiding yarn orientation can be determined by computing the projected length of one braider in the end view of the structure (points P1–P2 in Fig. 6), which is the projected length in a unit cell. Note that, although the angle of the braiders to the axial yarns remains constant and equal to α, it appears to vary on the top view in Fig. 6. This apparent variation occurs because the length of braider moving through the fabric has a different projected angle than one moving on the fabric surface. The projected length, L_p, equals

$$L_p = t\,\mathrm{cosec}\,\gamma + 2S_n(1 - \mathrm{cosec}\,\gamma) + 2S_a\cos\gamma \quad (15)$$

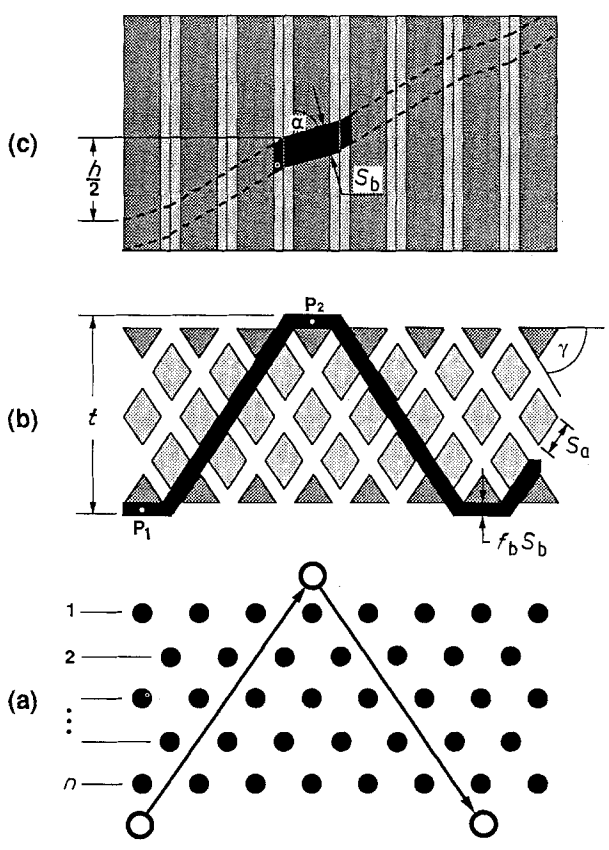

Figure 6 Path of one braiding yarn in fabric: (a) braid pattern; (b) end view; and (c) top view.

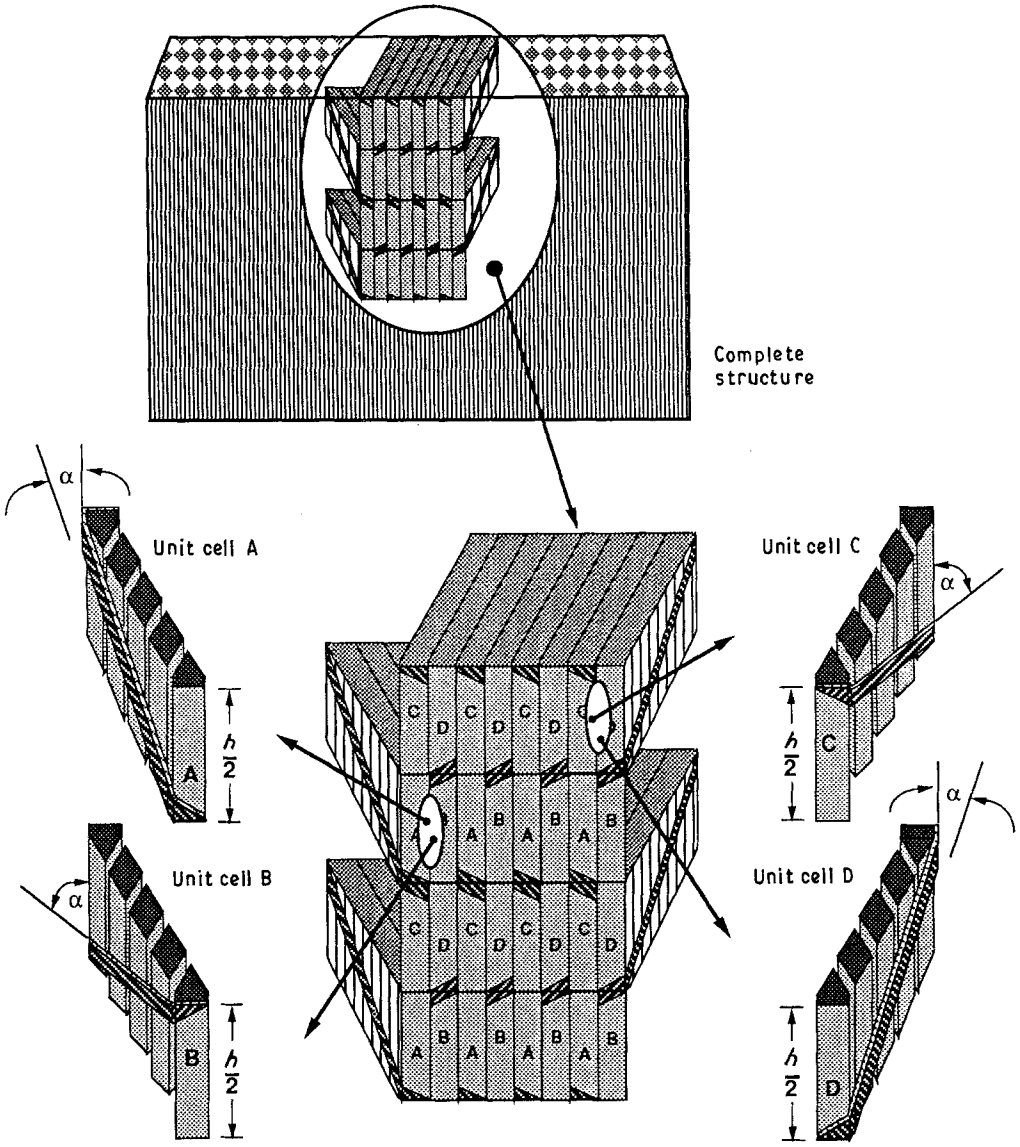

Figure 7 Unit cell model of three-dimensional fabric showing four symmetrical repeating cells. Each one includes a braiding yarn and a number of axial yarns.

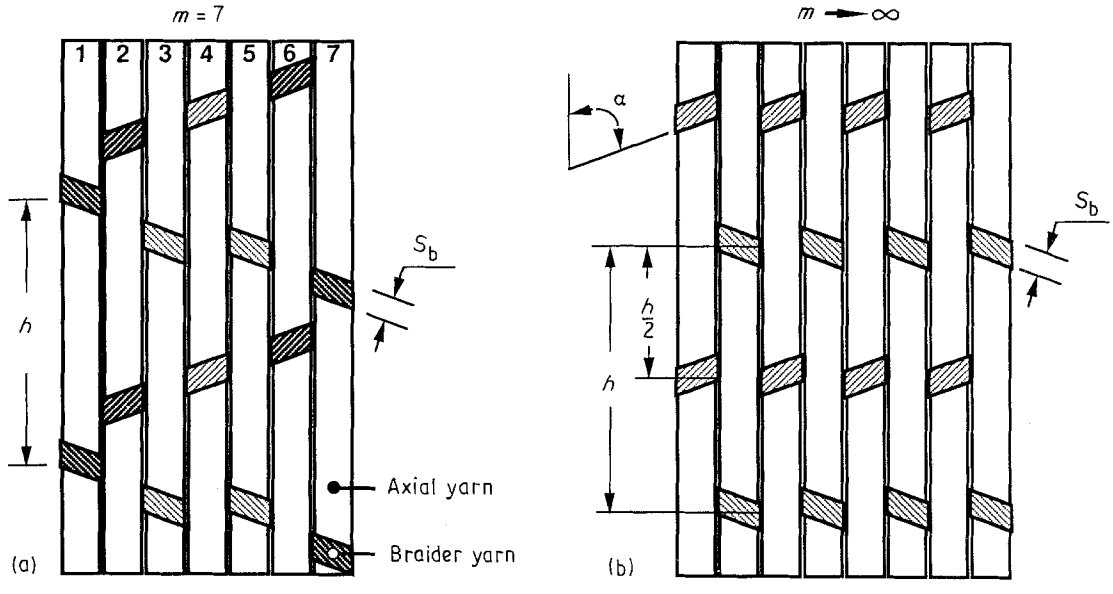

Figure 8 Effect of fabric width on braid geometry: (a) top view of finite-width preform; (b) infinite-width preform.

The braider yarn angle is then simply given by

$$\alpha = \tan^{-1}\left[\frac{2L_p}{h}\right] \quad (16)$$

The volume of each component in the structure can be determined by computing the total length of one braider in a unit cell.

$$L_b = \frac{L_p}{\sin\alpha} = \frac{h}{2\cos\alpha} \quad (17)$$

The volume of braiding yarn in a unit cell can be shown to equal

$$V_b = L_b f_b S_b^2 \quad (18)$$

Similarly, the volume of axial yarns in a unit cell equals

$$V_a = \frac{h}{2} S_a[(n-1)S_a\sin(2\gamma) + 4S_n\cos\gamma] \quad (19)$$

And the total volume of a unit cell equals

$$V_t = V_a + \frac{h}{2} f_b S_b[(n-1)S_a + L_p] \quad (20)$$

The fibre volume fraction, v_f (total fibre volume/unit cell volume), the braider fibre volume fraction, v_b (braider fibre volume/total fibre volume), and the volume fraction of the void space, v_v (volume of inter yarn voids/unit cell volume), can then easily be computed from Equations 21–23

$$v_f = \frac{V_a\kappa_a + V_b\kappa_b}{V_t} \quad (21)$$

$$v_b = \frac{V_b\kappa_b}{V_a\kappa_a + V_b\kappa_b} \quad (22)$$

$$v_v = 1 - \frac{V_a + V_b}{V_t} \quad (23)$$

2.5. Criterion for yarn jamming

The geometric structure of any three-dimensional fabric is limited significantly by the action of yarns jamming against each other. The model given in the previous section does not consider this limitation. When yarn jamming is included, the allowable fabric states are reduced. In this section, we develop the quantitative limits associated with this action in a two-step braid. It is interesting to notice that the mechanism of yarn jamming, although discussed frequently in the textile literature, is often neglected in the analysis of composites.

In two-step braids, the fabric geometry has no limits as the braider angle becomes very small. In that case, the braiders approach an array parallel to the axial yarns. However, as the pitch length is reduced, the braider angle increases, and a point is reached in which the yarns jam against each other. If all other parameters remain constant, the pitch length cannot be reduced further.

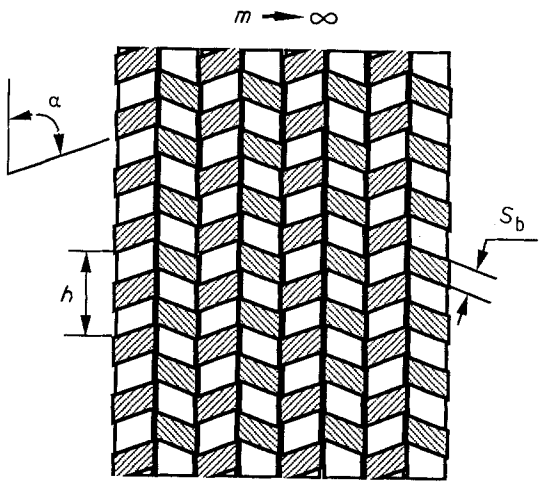

Figure 9 Surface geometry of braid at jamming point.

The point of jamming is shown in Fig. 9. Compare the unjammed view of Fig. 8b. The specific yarn-to-yarn contact point is shown, together with the pertinent fabric parameters. Surprisingly, this rather complex limiting fabric state can be described simply by

$$h_j = \frac{2S_b}{\sin\alpha} \quad (24)$$

where h_j denotes the pitch length at jamming point.

In a narrow or finite width structure, the geometry becomes considerably more complex due to end effects. Fig. 8a shows the yarn path for a structure seven columns wide. Note that the braider crossing points lie on an angled line. In an infinitely wide structure, Fig. 8b, these crossings lie perpendicular to the braiding direction. The jamming point as given above applies equally well to finite-width structures.

Owing to the end effect of finite-width structures, the orientation angle of all braiders are not equal. The braiders passing through the side face of the fabric will have less length in a braiding step. However, because all yarns are advanced at the same rate, the pitch lengths of all braiders are equal, and the "end" braiders will lie at a somewhat lower angle than those passing through the centre of the structure.

The point of jamming not only gives the boundary condition for the fabric model, it also provides an important process limitation. During braiding, it has been observed that, as long as the fabric is advanced fast enough to avoid jamming, the point of convergence is stable in space. Under this normal process condition, no beat-up mechanism is required, and the braid pitch length equals the braid take-up length in each machine step. If for any reason, the advance rate is reduced and the pitch length drops below the jamming level, the convergence point will automatically move closer to the braiding plane until no further braider motions are possible and the process breaks down. This condition occurs because the pitch length in the fabric becomes greater than the length advanced by the machine.

3. Experimental procedure

A number of two-step braids were made on laboratory-scale equipment similar to that shown in Fig. 1. The details of these samples are given in Table I. The bare fibre preforms (Braid I) were rectangular in cross-section, consisting of twelve-column by five-layer axial yarns (Kevlar® 49 with a linear density of 9.57×10^{-3} kg m^{-1}) and fifteen braiding yarns (Kevlar 49 with a linear density of 2.39×10^{-3} kg m^{-1}). The consolidated samples (Braid II) were also rectangular in cross-section, with seven-column, five-layer axial arrays and ten braiders as shown in Fig. 3. All axial yarns were made of Kevlar 29 with a linear density of 3.33×10^{-3} kg m^{-1} (30 000 denier, denier $= g/9000$ m) and 27 273 filaments. Kevlar 49 was used for the braiding yarns. They were much finer than the axial yarns with a linear density of 2.53×10^{-4} kg m^{-1} (2280 denier) and 2072 filaments.

The braided preforms (Braid II) were inserted into a metal mould and impregnated with a polymeric matrix by resin transfer moulding. The epoxy resin system used consisted of a mixture of 70 parts of Epon® Resin 9405 by weight and 30 parts of Epon Curing Agent® 9470. Both the metal mould and resin mixture were preheated to 100 °C. The resin was injected into one end of the preform under pressure while the other end was subjected to vacuum. Although the fabric was quite dense, the resin flowed throughout the preform. The impregnated material was held in the mould at 150 °C for 3 h to cure the resin.

It was observed that the preform surface, which was relatively rough, followed the general contour of Fig. 4. After consolidation, the surface was flat, resembling that shown in Fig. 5.

Cross-sections of samples after impregnation (Braid II) are shown in Fig. 10. These photomicrographs confirm the basic assumptions regarding the shape and packing of the component yarns. The axial yarns were clearly diamond shaped and the braiders were approximately rectangular. The cross-sections were evaluated on a computer-based image analyser to determine the level of fibre packing. As shown in Table I, the yarn packing fraction was found to average 0.70 for the bare fibre preforms (Braid I) and 0.78 for the consolidated composites (Braid II).

Fibre volume fraction was determined from measured dimensions and component weights. Fibre orientation and yarn aspect ratio were measured from the photomicrographs.

4. Results and discussion

Using the equations developed in the analysis, we established the key relations between process variables and fabric geometry. Some of these results were compared with measured values, as will be discussed. In addition, we found that the range of allowable fabric structures for this type of braid is limited to special parameter combinations, as dictated by effects such as yarn jamming and fibre packing.

The microgeometric parameters of the test samples were compared with computed values and are summarized in Table I. Both a bare fibre preform and a consolidated composite are included. Note that these materials differ in both yarn size and braid pattern. There was excellent agreement between measured and predicted levels of fabric dimensions, fibre orientation, and fibre volume fraction. The relatively high levels of fibre volume fraction for both the preform and composite are characteristic of this type of structure. The experiments reported are not intended to cover a wide range of variables, but rather to confirm the validity of the model developed.

The results of the geometric analysis can be represented in many ways, and the selection of relations evaluated depends on the specific technical need. We have focused on fibre orientation angle and fibre volume fraction to describe the braid geometry. The relationship between these variables and the process parameters is shown in Figs 11–15. All variables are given in dimensionless form, and in each case show a number of variables were fixed.

The fibre volume fraction relation in Fig. 11 shows that for the fixed parameters selected, only a limited window exists for this type of fabric construction. The window is bounded by two factors: yarn jamming and the point of zero braid angle. Fabric constructions corresponding to the curved line marked "jamming" are at their tightest allowable point, and constructions at the $\alpha = 0$ curve have infinite pitch length. As the

TABLE I Theoretical and experimental results

Parameters	Braid I (preform)		Braid II (composite)	
	Measured	Computed	Measured	Computed
λ_a(g m^{-1})	9.57		3.33	
λ_b(g m^{-1})	2.39		0.25	
m	12		7	
n	5		5	
h (mm)	17.8		4.98	
f_a	0.78		1.32	
f_b	0.12		0.05	
κ_a	0.70		0.78	
κ_b	0.70		0.78	
t (mm)	9.0	8.9	7.0	7.3
w (mm)	63.0	62.9	15.0	14.6
α (deg)	65.0	65.9	75.0	76.7
v_f (%)	56.0	56.8	73.0	73.6

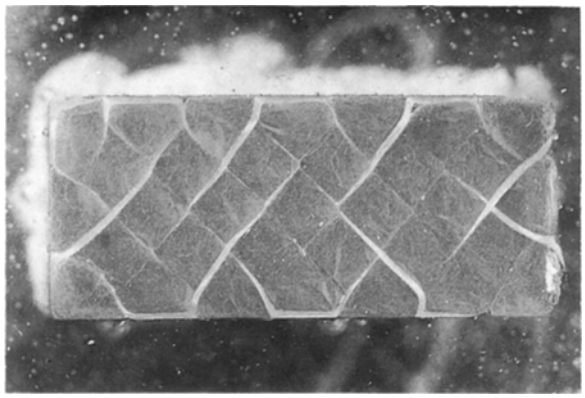

Figure 10 Photograph of a cross-section of braided consolidated composite (Braid II in Table I).

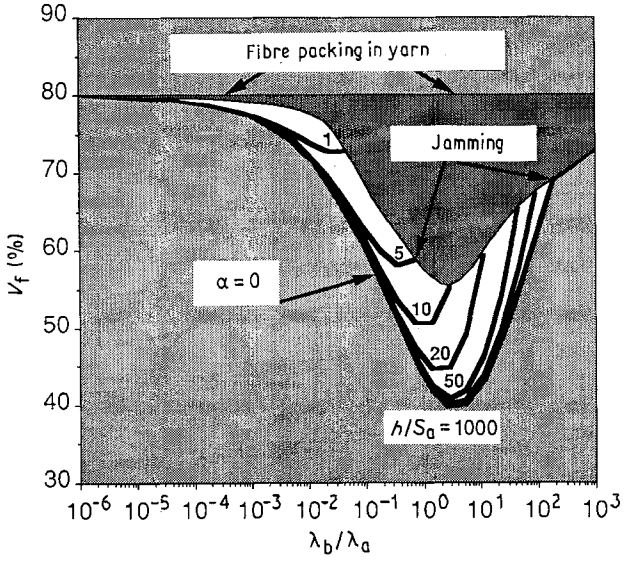

Figure 11 Fibre volume fraction plotted versus ratio of braider-to-axial linear density. Allowable process window is shown ($\kappa_a = 0.8$, $\kappa_b = 0.8$, $\gamma = 38°$, $f_b = 0.2$, $n = 5$).

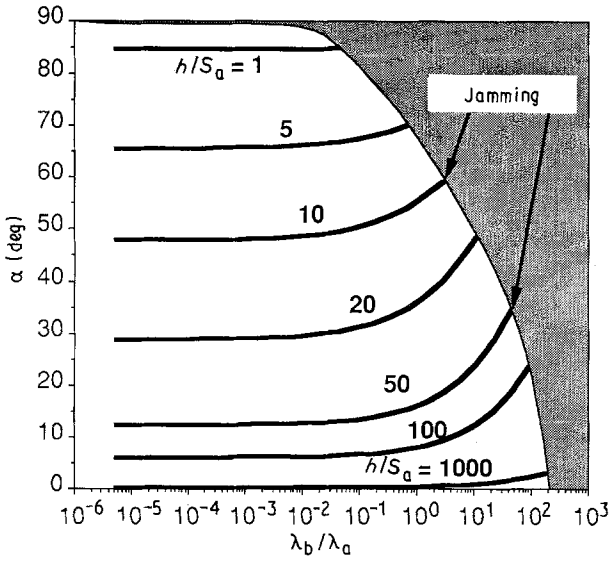

Figure 12 Fibre orientation angle versus ratio of braider-to-axial yarn linear density. Allowable process window is shown ($\kappa_a = 0.8$, $\kappa_b = 0.8$, $\gamma = 38°$, $f_b = 0.2$, $n = 5$).

pitch length h/S_a increases, the fibre volume fraction decreases as shown. Increasing the ratio of braider-to-axial linear density causes the maximum allowed fibre volume fraction, which is limited by jamming, to go through a minimum. At fixed levels of pitch length, an increase in this ratio generally causes the fibre volume fraction to decrease because the inclusion of larger braiding yarns creates more voids. However, at large ratios above approximately 3, an increase in ratio gives a higher fibre volume fraction. At a ratio of about 200, the fabric reaches a curious limit in which the braiders are jammed at a very low angle. The fibre packing in the yarns, taken as 0.8, limits the maximum fibre volume fraction in the fabric. The degree to which the yarns pack in a fabric, the yarn volume

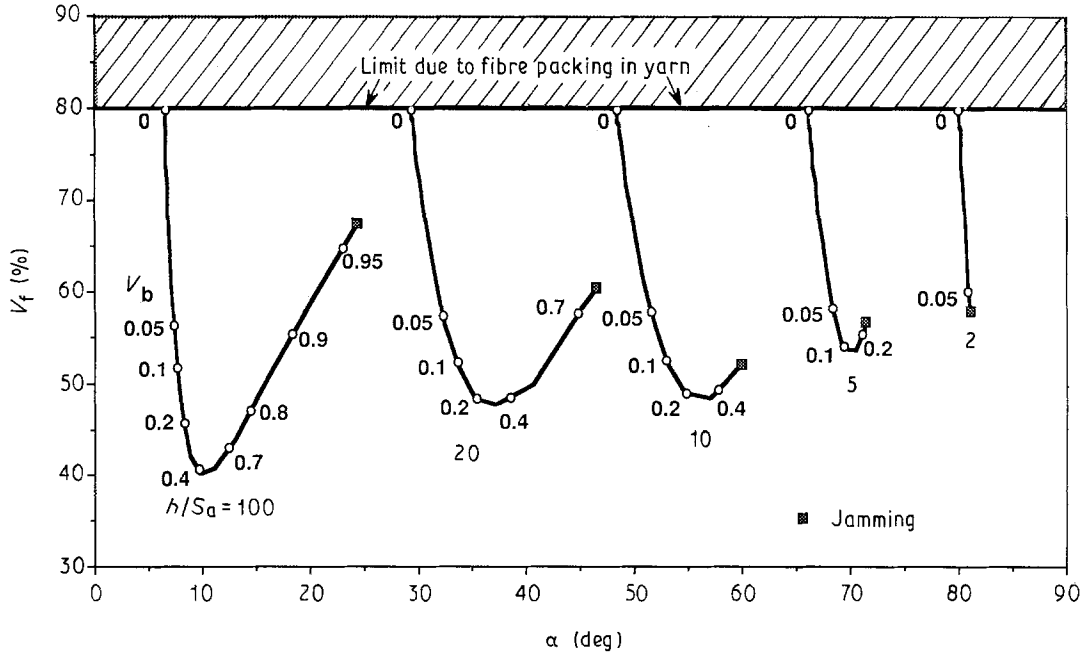

Figure 13 Property map of fibre volume fraction and fibre orientation angle for varying pitch length and fraction of braiding fibres ($\kappa_a = 0.8$, $\kappa_b = 0.8$, $\gamma = 38°$, $f_b = 0.2$, $n = 5$).

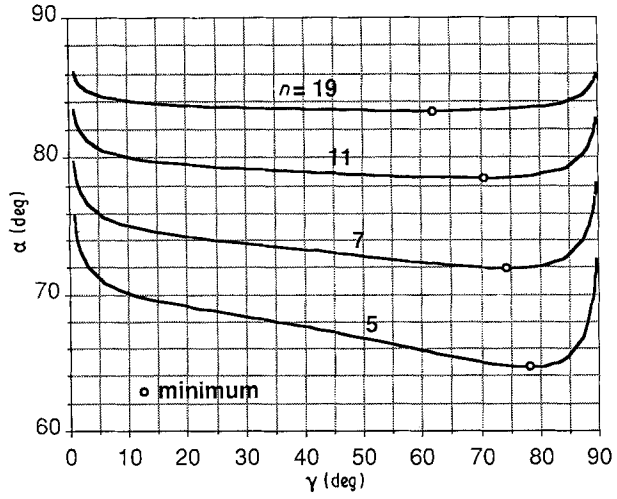

Figure 14 Effect of inclination angle of braiders to braiding plane on the spatial orientation angle ($\kappa_a = 0.8$, $\kappa_b = 0.8$, $f_b = 0.2$, $\lambda_b/\lambda_a = 0.1$, $h/S_a = 5$).

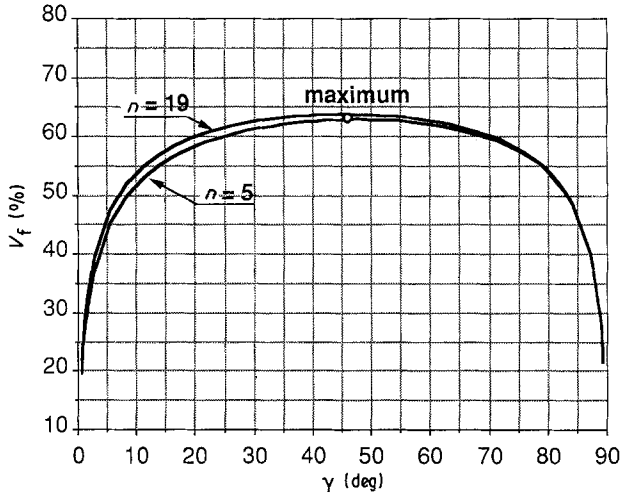

Figure 15 Effect of inclination angle of braiders to braiding plane on the fibre volume fraction ($\kappa_a = 0.8$, $\kappa_b = 0.8$, $f_b = 0.2$, $\lambda_b/\lambda_a = 0.1$, $h/S_a = 5$).

fraction, can be determined from the plots shown simply by dividing the indicated fibre volume fraction by the fibre packing factor.

The orientation angle is plotted against the same parameters in Fig. 12. As expected, increasing the pitch length reduces this angle. The linear density ratio of braiders-to-axials has a relatively low effect below a level of unity. Above this point, increasing the size of braider yarns increases fibre angle especially at higher pitch lengths. Jamming limits the allowable fabric geometries as the braiders increase in size and the pitch length decreases.

A property map of fibre volume fraction and orientation angle is shown in Fig. 13 for fixed levels of several parameters. As the pitch length increases, the orientation angle decreases and the fibre volume fraction remains about constant. For a fixed pitch, as the fraction of braiding fibres increases, the variables change as shown until the yarns jam. This property map indicates that a wide range of orientation angle and fibre volume fraction can be achieved by varying the pitch and the relative amount of braiding fibres used. This map provides guidance in designing a fabric for a particular application.

The inclination angle of the braiders, γ, shown in Fig. 6, can be used to adjust the fabric geometry. In most cases, when the braiders are pulled tight, this angle tends to be close to 45°. However, it can be varied during braiding by a forming plate or afterwards by adjusting the dimensions of a mould. Changing the inclination angle permits the fabric dimensions to be adjusted and the microgeometry to be altered.

The effect of changes in inclination angle on orientation angle is shown in Fig. 14. Increasing the inclination causes the orientation angle to go through a minimum at about 80° for a five-layer braid. As the number of layers increases, the orientation angle increases and the minimum shifts to the left.

The fibre volume fraction is also affected by the inclination angle as shown in Fig. 15. It goes through a maximum at about 45°. The number of layers essentially has no effect on this variable.

5. Conclusions

We draw the following conclusions from the analytical and experimental work.

1. The unit cell approach has been used effectively to define the geometric relations describing the complex three-dimensional geometry of two-step braids.

2. Preliminary experiments confirm the basic mathematical predictions.

3. The two-step braid can be made in a wide range of geometric patterns by adjusting the key parameters of ratio of braider-to-axial yarn linear density, pitch length during braiding, inclination angle, and number of braiding layers. Generally high fibre volume fractions are possible (up to 75%), and generally high orientation angles result when the fabric is close to the point of jamming.

4. This braid, as most textile structures, can be made only in a limited process window (as shown in Figs 11–13). The factors limiting the allowable structures are yarn jamming and the point of zero orientation angle.

5. The fibre orientation, α, and volume fraction, v_f, can readily be adjusted by increasing the following variables:

(a) pitch length h, which reduces both α and v_f;

(b) ratio of braider-to-axial linear density λ_b/λ_a, which decreases v_f at low ratios and increases it at high ratios;

(c) inclination angle, γ, which adjusts α through a minimum and v_f through a maximum;

(d) number of layers n, which increases α;

(e) braider thickness-to-width ratio, f_b, which increases the jamming angle.

6. The fibre packing in two-step braids forms prismatic axial yarns and rectangular braiding yarns.

Acknowledgement

One of the authors (T. W. C.) thanks the partial support of the US Army Research Office through the

University Research Initiative programme at the Center for Composite Materials of the University of Delaware.

References

1. P. POPPER and R. F. McCONNELL, US Pat. 4719837, January 1988.
2. R. D. WELLER, "AYPEX: A New Method of Composite Reinforcement Braiding", 3-D Composite Materials, NASA Conference Publication 2420, November 1985.
3. P. M. COLE, US Pat. 4737 399, 1988.
4. R. FLORENTINE, US Pat. 4312261, January 1982.
5. W. LI and A. EL SHIEKH, *SAMPE Q.* **19** (1988) 22.
6. F. K. KO, H. B. SOEBROTO and C. LEI, "3-D Net Shaped Composites by the two-step Braiding Process", in 33rd International SAMPE Symposium Vol. **33** (March 1988) pp. 912–21.
7. T. J. WHITNEY, Master Thesis, University of Delaware (1988).
8. J. W. S. HEARLE, P. GROSBERG and S. BACKER, "Structural Mechanics of Fibers, Yarns, and Fabrics", Vol. 1 (Wiley-Interscience, 1969) p. 80.
9. F. T. PEIRCE, *J. Text. Inst.* **28** (1937) T45.
10. D. BRUNNSCHWEILER, *ibid.* **45** (1954) T55.
11. J. W. S. HEARLE, P. GROSBERG and S. BACKER, "Structural Mechanics of Fibers, Yarns, and Fabrics", Vol. **1** (Wiley-Interscience, 1969) p. 323.

Received 2 January
and accepted 4 September 1990